Blood testing at the single cell level using quantitative phase and amplitude microscopy

Mustafa Mir,[1,*] Krishnarao Tangella,[2] and Gabriel Popescu[1]

[1]*Quantitative Light Imaging Laboratory, Department of Electrical and Computer Engineering,, Beckman Institute for Advanced Science and Technology, University of Illinois at Urbana-Champaign, 405 N. Matthews Ave., Urbana, IL 61801, USA*

[2]*Department of Pathology, Christie Clinic and University of Illinois at Urbana-Champaign, 1400 W. Park St., Urbana, IL 61801, USA*

**mmir2@illinois.edu*

Abstract: It has recently been shown that quantitative phase imaging methods can provide clinically relevant parameters for red blood cell analysis with unprecedented detail and sensitivity. Since the quantitative phase information is dependent on both the thickness and refractive index, a major limitation to clinical translation has been a simple and practical approach to measure both simultaneously. Here we demonstrate both theoretically and experimentally that, by combining quantitative phase with a single absorption measurement, it is possible to measure both quantities at the single cell level. We validate this approach by comparing our results to those acquired using a clinical blood analyzer. This approach to decouple the thickness and refractive index for red blood cells may be used with any quantitative phase imaging method that can operate in tandem with bright field microscopy at the Soret-band wavelength.

OCIS codes: (170.0180) Microscopy; (170.1470) Blood or tissue constituent monitoring; (170.1530) Cell analysis; (170.1610) Clinical applications; (300.1030) Absorption; (180.3170) Interference microscopy

References and links

1. B. J. Bain, *Blood Cells A Practical Guide*, 3rd ed. (Blackwell Science, London, 2002).
2. B. J. Bain, "Diagnosis from the blood smear," N. Engl. J. Med. **353**(5), 498–507 (2005).
3. H. H. Billett, M. E. Fabry, and R. L. Nagel, "Hemoglobin distribution width: a rapid assessment of dense red cells in the steady state and during painful crisis in sickle cell anemia," J. Lab. Clin. Med. **112**(3), 339–344 (1988).
4. M. Piagnerelli, K. Zouaoui Boudjeltia, D. Brohee, A. Vereerstraeten, P. Piro, J.-L. Vincent, and M. Vanhaeverbeek, "Assessment of erythrocyte shape by flow cytometry techniques," J. Clin. Pathol. **60**(5), 549–554 (2007).
5. G. Rusciano, "Experimental analysis of Hb oxy-deoxy transition in single optically stretched red blood cells," Phys. Med. **26**(4), 233–239 (2010).
6. S. Winoto-Morbach, W. Müller-Ruchholtz, and V. Tchikov, "Magnetophoresis: II. Quantification of iron and hemoglobin content at the single erythrocyte level," J. Clin. Lab. Anal. **9**(1), 42–46 (1995).
7. A. Esposito, T. Tiffert, J. M. Mauritz, S. Schlachter, L. H. Bannister, C. F. Kaminski, and V. L. Lew, "FRET imaging of hemoglobin concentration in Plasmodium falciparum-infected red cells," PLoS ONE **3**(11), e3780 (2008).
8. K. A. Sem'yanov, P. A. Tarasov, J. T. Soini, A. K. Petrov, and V. P. Maltsev, "Calibration-free method to determine the size and hemoglobin concentration of individual red blood cells from light scattering," Appl. Opt. **39**(31), 5884–5889 (2000).
9. M. Mir, Z. Wang, Z. Shen, M. Bednarz, R. Bashir, I. Golding, S. G. Prasanth, and G. Popescu, "Optical measurement of cycle-dependent cell growth," Proc. Natl. Acad. Sci. U.S.A. **108**(32), 13124–13129 (2011).
10. M. Mir, Z. Wang, K. Tangella, and G. Popescu, "Diffraction phase cytometry: blood on a CD-ROM," Opt. Express **17**(4), 2579–2585 (2009).
11. Y. Park, C. A. Best, T. Auth, N. S. Gov, S. A. Safran, G. Popescu, S. Suresh, and M. S. Feld, "Metabolic remodeling of the human red blood cell membrane," Proc. Natl. Acad. Sci. U.S.A. **107**(4), 1289–1294 (2010).
12. Y. Park, C. A. Best, K. Badizadegan, R. R. Dasari, M. S. Feld, T. Kuriabova, M. L. Henle, A. J. Levine, and G. Popescu, "Measurement of red blood cell mechanics during morphological changes," Proc. Natl. Acad. Sci. U.S.A. **107**(15), 6731–6736 (2010).
13. Y. Park, M. Diez-Silva, D. Fu, G. Popescu, W. Choi, I. Barman, S. Suresh, and M. S. Feld, "Static and dynamic light scattering of healthy and malaria-parasite invaded red blood cells," J. Biomed. Opt. **15**(2), 020506 (2010).

#155401 - $15.00 USD Received 27 Sep 2011; revised 21 Oct 2011; accepted 6 Nov 2011; published 7 Nov 2011

14. G. Popescu, Y. Park, R. R. Dasari, K. Badizadegan, and M. S. Feld, "Coherence properties of red blood cell membrane motions," Phys. Rev. E Stat. Nonlin. Soft Matter Phys. **76**(3), 031902 (2007).
15. G. Popescu, Y. Park, N. Lue, C. Best-Popescu, L. Deflores, R. R. Dasari, M. S. Feld, and K. Badizadegan, "Optical imaging of cell mass and growth dynamics," Am. J. Physiol. Cell Physiol. **295**(2), C538–C544 (2008).
16. G. Popescu, K. Badizadegan, R. R. Dasari, and M. S. Feld, "Observation of dynamic subdomains in red blood cells," J. Biomed. Opt. **11**(4), 040503 (2006).
17. S. Seo, S. O. Isikman, I. Sencan, O. Mudanyali, T. W. Su, W. Bishara, A. Erlinger, and A. Ozcan, "High-throughput lens-free blood analysis on a chip," Anal. Chem. **82**(11), 4621–4627 (2010).
18. S. Seo, T. W. Su, D. K. Tseng, A. Erlinger, and A. Ozcan, "Lensfree holographic imaging for on-chip cytometry and diagnostics," Lab Chip **9**(6), 777–787 (2009).
19. N. T. Shaked, L. L. Satterwhite, M. J. Telen, G. A. Truskey, and A. Wax, "Quantitative microscopy and nanoscopy of sickle red blood cells performed by wide field digital interferometry," J. Biomed. Opt. **16**(3), 030506 (2011).
20. A. R. Brazhe, A. I. Yusipovich, E. Y. Parshina, N. Y. Brysgalova, N. A. Brazhe, A. G. Lomakin, G. G. Levin, and G. V. Maksimov, "Laser interference microscopy in erythrocyte study," J. Appl. Phys. **105**, 102037(2009).
21. M. Mir, H. Ding, Z. Wang, J. Reedy, K. Tangella, and G. Popescu, "Blood screening using diffraction phase cytometry," J. Biomed. Opt. **15**(2), 027016 (2010).
22. B. Rappaz, A. Barbul, Y. Emery, R. Korenstein, C. Depeursinge, P. J. Magistretti, and P. Marquet, "Comparative study of human erythrocytes by digital holographic microscopy, confocal microscopy, and impedance volume analyzer," Cytometry A **73A**(10), 895–903 (2008).
23. B. Rappaz, F. Charrière, C. Depeursinge, P. J. Magistretti, and P. Marquet, "Simultaneous cell morphometry and refractive index measurement with dual-wavelength digital holographic microscopy and dye-enhanced dispersion of perfusion medium," Opt. Lett. **33**(7), 744–746 (2008).
24. B. Rappaz, P. Marquet, E. Cuche, Y. Emery, C. Depeursinge, and P. Magistretti, "Measurement of the integral refractive index and dynamic cell morphometry of living cells with digital holographic microscopy," Opt. Express **13**(23), 9361–9373 (2005).
25. Y. K. Park, T. Yamauchi, W. Choi, R. Dasari, and M. S. Feld, "Spectroscopic phase microscopy for quantifying hemoglobin concentrations in intact red blood cells," Opt. Lett. **34**(23), 3668–3670 (2009).
26. Z. Wang, L. Millet, M. Mir, H. Ding, S. Unarunotai, J. Rogers, M. U. Gillette, and G. Popescu, "Spatial light interference microscopy (SLIM)," Opt. Express **19**(2), 1016–1026 (2011).
27. Z. Wang and G. Popescu, "Quantitative phase imaging with broadband fields," Appl. Phys. Lett. **96**(5), 051117 (2010).
28. R. Barer, "Refractometry and interferometry of living cells," J. Opt. Soc. Am. **47**(6), 545–556 (1957).
29. R. Barer, J. B. Howie, K. F. Ross, and S. Tkaczyk, "Applications of refractometry in haematology," J. Physiol. **120**(4), 67P–68P (1953).
30. R. Barer and K. A. Ross, "Refractometry of living cells," J. Physiol. **118**(2), 38P–39P (1952).
31. R. Barer and S. Tkaczyk, "Refractive index of concentrated protein solutions," Nature **173**(4409), 821–822 (1954).
32. Z. Wang, I. S. Chun, X. Li, Z. Y. Ong, E. Pop, L. Millet, M. U. Gillette, and G. Popescu, "Topography and refractometry of nanostructures using spatial light interference microscopy," Opt. Lett. **35**(2), 208–210 (2010).
33. S. Prahl, "Tabulated molar extinction coefficient for hemoglobin in water" (1998), *http://omlc.ogi.edu/spectra/hemoglobin/summary.html*.

1. Introduction

Current clinical technologies for analyzing red blood cells have remained essentially unchanged since the invention of impedance counters and flow cytometers. Although these methods provide high throughput measurements, the information provided is generally limited to population level statistics for morphology and bulk measurement in the case of hemoglobin concentration [1,2]. Even though automated counters have been developed to provide statistical information on both hemoglobin concentration distributions and general morphological information [3,4], they lack the resolution required to aid in a differential diagnosis. These limitations mean that if an abnormality is detected by an automated counter, pathologists must rely on manual qualitative analysis of blood smears for information on single cells. Furthermore, automated counters are expensive, bulky and costly to maintain making them unsuitable as a point of care diagnostic tool. Since the measurement of hemoglobin is of fundamental importance to blood analysis, several techniques such as Raman Imaging [5], magnetophoresis and gravitation sedimentation [6], FRET based sensing [7] and scattering based measurements [8] among many others have been developed. However, these methods also require complicated sample preparation or measurement procedures.

It has recently been demonstrated that quantitative phase imaging (QPI) is capable of providing detailed, quantitative, morphological analysis as well as several novel clinically

#155401 - $15.00 USD Received 27 Sep 2011; revised 21 Oct 2011; accepted 6 Nov 2011; published 7 Nov 2011

relevant parameters for red blood cells [9–20] at the single cell level. However, since the optical phase shift through a red blood cell is a function of both thickness and refractive index, the demonstrated morphological analysis has depended on *a priori* knowledge of the hemoglobin concentration [10,21]. Other groups utilizing phase measurements have addressed this problem in various manners. One popular approach utilizes two different immersion media to decouple the thickness and refractive index [22–24]. This approach requires that cells be kept in place as the media is changed and thus requires coating of the cover slips and a profusion setup. Thus, such a technique may not be well suited for clinical measurements especially with the goal of developing a point of care diagnostic tool in mind. More recently, it has been demonstrated that by acquiring diffraction phase microscope (DPM) measurements at different wavelengths, hemoglobin concentration may be quantified at the single cell level [25]. This technique, dubbed Spectroscopic Phase Microscopy, is highly stable and utilizes a relatively simple experimental setup and is therefore well suited for adoption as a clinical method. However, DPM requires modifications to the illumination path of a microscope and is not easily integrated with other popular modalities such as fluorescence measurements.

Here we provide the proof of principle of a novel combination of the *quantitative phase* information measured using a Spatial Light Interference Microscope (SLIM) [26,27], with a *bright field absorption* measurement acquired in the Soret band. We show both theoretically and experimentally, that this combination can be used to quantitatively determine both hemoglobin concentration and cell morphology at the single cell level. SLIM is a new QPI modality which utilizes broadband illumination (400-700 nm, center wavelength of 530 nm) in common path geometry. Due to this SLIM provides the ability to measure optical path length with unparalleled sensitivities of 0.28 nm spatially and 0.029 nm temporally [16]. Furthermore, SLIM is designed as an add-on module to a commercial microscope and can easily be integrated with other commonly used modalities.

The method described here may be deployed as a standalone blood smear analyzer in a clinical setting without relying on external measurements of hemoglobin concentrations. The additional set of measured parameters may offer insight into the nature of morphological abnormalities used to identify various disorders and will likely automate the diagnosis of conditions that currently require manual smear analysis. Such a method may be implemented for a fraction of the cost of current analyzers, requires no reagents or complicated sample preparation and has the potential to easily be adapted to a compact and portable platform [10,17]. The technique presented here may be also utilized with any QPI instrument, provided that it meets the resolution and sensitivity requirements for single erythrocyte analysis.

2. Theory

The phase measured by SLIM is related to the refractive index and thickness of the sample as

$$\Delta\phi(x,y) = k_0 \Delta n(x,y) t(x,y) \tag{1}$$

where $k_0 = 2\pi/\lambda$ and λ is the mean wavelength, t is the thickness, and $\Delta n = (\beta C + n_w) - n_s$. Here β is the refractive increment of protein in mL/g, C is the concentration in g/mL, n_w is refractive index of water and n_s is the refractive index of the surrounding media. The refractive increment is defined as the increase in refractive index per one percent increase in the concentration [28–31]. It was shown in the 1950s that the refractive increments of a wide range of proteins lie within the range of 0.17 and 0.20 [28–31]. Furthermore, this is also true for other cellular components such as lipids and carbohydrates to the point that we may assume that the bulk refractive index of a living cell is a good measure of the total dry mass of the cell [17–21]. Given the small variations in refractive increment Eq. (1) can be rewritten in terms of the concentration and refractive increment as

$$\Delta\phi(x,y) = k_0 \left[\beta C(x,y) + \Delta n_{ws}\right] t(x,y) \tag{2}$$

where $\Delta n_{ws} = n_w - n_s$ is the difference between the refractive index of water and the surrounding media. The absorption measurements may be described according to the Lambert-Beer law:

#155401 - $15.00 USD Received 27 Sep 2011; revised 21 Oct 2011; accepted 6 Nov 2011; published 7 Nov 2011

$$A = -\ln\left(\frac{I}{I_0}\right) = \sigma t N \tag{3}$$

where A is absorbance, σ is the absorption cross section perpendicular to the optical axis and N is the density of absorbers. The relationship between absorption cross section, density and refractive index is $\sigma N = 2k_0 n''$, where n'' is the imaginary part of the refractive index which describes the absorption phenomenon. For liquid solutions the absorbance is typically expressed in terms of a molar extinction coefficient:

$$A'(x,y) = -\log_{10}\left(\frac{I}{I_0}\right) = \frac{\varepsilon t(x,y) C(x,y)}{M} \tag{4}$$

where ε is molar extinction coefficient in $L \cdot mol^{-1} cm^{-1}$ at the wavelength being used, M is the molar mass (g/mol) and C is the concentration (g/L). It can be seen that the only unknowns in Eq. (2) and Eq. (3) are the thickness, t and concentration C. Therefore we may simply solve for both:

$$C(x,y) = \frac{\Delta n_{ws}}{\frac{\varepsilon}{M k_0}\frac{\Delta\phi(x,y)}{A'(x,y)} - \beta} \tag{5}$$

$$t(x,y) = \frac{M A'(x,y)}{\varepsilon C(x,y)} \tag{6}$$

Thus, for a single molecular species case, as in the case of the almost homogenous red blood cell, only one absorption and one phase measurement is necessary to determine both the thickness and the concentration.

3. Materials and methods

3.1. Sample preparation

Blood is drawn from patients at a local hospital by venipuncture and stored in EDTA coated containers at room temperature. A complete blood count (CBC) analysis is then performed on each sample using a clinical impedance counter (Coulter LH50, Beckman Coulter). This counter is used daily for routine analysis at the hospital's hematology laboratory. To comply with HIPAA and University of Illinois Internal review board regulations each sample is marked with a unique identifier and all personal patient information is removed prior to transferring the samples to the university laboratory. Prior to imaging, the whole blood is diluted with Coulter LH series diluent (Beckman-Coulter) to a concentration of 0.2% whole blood in solution. This is the same diluent that is used by the impedance counter and fixes the cells morphology to prevent errors caused by flow in the measurement apparatus of the impedance counter. We use this diluent so that any effects that it does have on the morphology are also present in our measurements, such that a comparison with the clinical analyzer is possible. For imaging, a sample chamber is created by punching a hole in double sided scotch tape and sticking one side of the tape onto a cover slip. The sample is then pipetted into the chamber created by the hole and it is sealed on the top using another cover slip [21]. The cells are allowed to settle for 5 minutes prior to measurement. This sealed chamber allows control over the sample volume, prevents drying and reduces cell translation. This method provides uniform samples, which are quick and easy to prepare and is well suited for bench-top, proof of principle studies.

3.2. Imaging

For measuring the quantitative phase map, SLIM is used, which has been described in detail previously [26,27]. The capabilities of SLIM have already been demonstrated in several

#155401 - $15.00 USD Received 27 Sep 2011; revised 21 Oct 2011; accepted 6 Nov 2011; published 7 Nov 2011

contexts ranging from cell dry mass measurements to measuring intracellular transport [9,32]. As shown in Fig. 1, SLIM is designed as an add-on module to a commercial phase contrast microscope (Zeiss Axio Observer Z1). For conventional phase contrast microscopy, a phase ring in the back focal plane of the objective is used to impart a $\pi/2$ phase shift to the un-scattered light, relative to the scattered light. For SLIM, the back focal plane of the phase contrast objective is projected onto a liquid crystal phase modulator which is used to impart additional phase shifts to the un-scattered light in increments of $\pi/2$. In total 4 intensity images are recorded corresponding to phase differences of 0, $\pi/2$, π and $3\pi/2$. A quantitative phase map may then be uniquely determined from these 4 images as previously described [26,27]. To ensure that the phase measured is integrated over the entire thickness of the cell we used a low numerical aperture (NA) objective. Thus, for both the SLIM and absorption measurements a 10x/0.3 Ph1 objective was used. The exposure time for each of the intensity maps is 15 milliseconds and a total of 0.75 second is required to acquire the 4 maps.

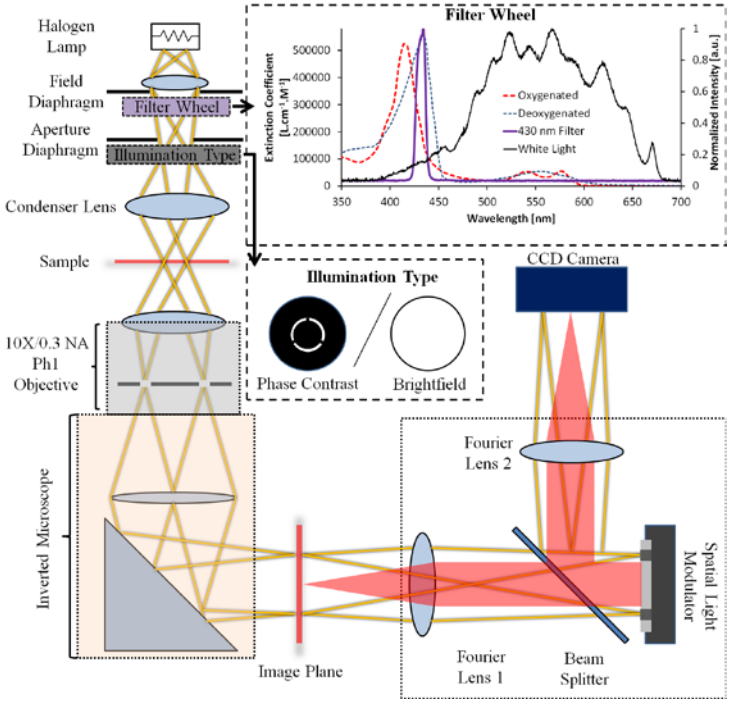

Fig. 1. Experimental setup. The SLIM system is built as an add-on module to a commercial phase contrast microscope. The back focal plane of the objective is projected onto a spatial light modulator which is calibrated to impart a phase shift to the un-scattered light (yellow lines) relative to the scattered light (shown in red). Four intensity images are recorded corresponding to 4 phase shifts in increments of $\pi/2$, the quantitative phase map is reconstructed from these 4 intensity images as detailed in Ref. [26]. For the SLIM measurements the illumination type is set to phase contrast and the filter wheel is set to an open position such that the entire spectrum of the halogen lamp is passed. For the absorption measurements the illumination type is set to bright field and a 430 nm filter is used in the filter wheel. The inset for the filter wheel shows the normalized intensity of the white light spectrum, the spectrum of the 430 nm bandpass filter (right axis) and the extinction coefficients of oxygenated and deoxygenated hemoglobin (left axis) as a function of wavelength from Ref. [33].

For measuring the absorption map a bandpass filter centered at 430 nm (+/– 10 nm) is introduced into the light path after the condenser field diaphragm as shown in Fig. 1. In principle any bandpass filter could be used, provided the SNR is high enough. The choice of 430 nm was made since it is strongly absorbed by both oxygenated and deoxygenated hemoglobin. . The phase contrast annulus in the condenser is also swung out of position so

#155401 - $15.00 USD Received 27 Sep 2011; revised 21 Oct 2011; accepted 6 Nov 2011; published 7 Nov 2011

that the illumination is set for bright-field measurements. In order to optimize the absorption measurement, both the NA of the condenser and the objective must be taken into account. As for the SLIM measurement the NA of the objective must be chosen such that the depth of field is greater than the thickness of the red blood cells. The optimal NA for the condenser was determined experimentally by varying NA between 0.55 and 0.1 and measuring the absorption. It was found for multiple objectives (data not shown) that the absorption continues to increase as the NA is decreased and peaks at a value close to the NA of the objective being used. After this point, aberrations become clearly observable in the image. For the 10x/0.3 objective used here, the value for the condenser NA which gave the greatest contrast was determined to be 0.2. For the absorption measurements an exposure time of 250 milliseconds is used. For each patient a 1.55 x 1.01 mm area is scanned corresponding to a 4x4 mosaic. When taking into account the time required for moving the stage and switching from SLIM to brightfield it takes approximately 2 minutes to measure each patient.

Although in principle any QPI technique could be coupled with an absorption measurement to yield results similar to those shown here, we used SLIM for two main reasons. First, the white light illumination used for SLIM allows for easy integration of a filter wheel into the setup to perform absorption measurements. Second, SLIM provides the lowest noise and highest sensitivities out of any QPI technique that we are aware of.

3.2. Data analysis

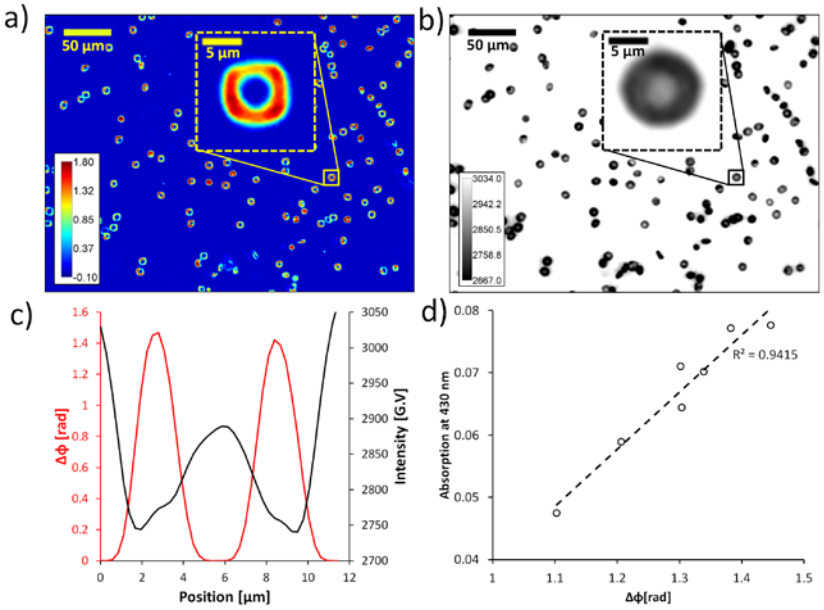

Fig. 2. Image analysis (a) Quantitative phase map acquired using SLIM, color bar is in radians. (b) Absorption map acquired at 430 nm, color bar is in 16-bit gray scale values. (a-b) Insets show an example of a single RBC from the maps. (c) Overlay of l line profiles drawn through the center of a single cell, the phase values are shown in red against the left axis and the corresponding intensity from the absorption maps are shown in black against the right axis. (d) Average absorption vs. phase for each of the 7 patients analyzed in this study, a strong linear relationship (dotted line) indicates the feasibility of this method. For the cell shown here the volume and hemoglobin concentration were calculated to be 86.18 fL and 0.3 g/mL respectively.

To analyze the images, a semi-automatic image routine was developed in MATLAB. A user selects several cells in every image, avoiding cells that are turned on their side or appear otherwise damaged. Using this routine it takes approximately 5 minutes to analyze the data from one patient. Once a cell is picked the region occupied by the cell is identified by

#155401 - $15.00 USD Received 27 Sep 2011; revised 21 Oct 2011; accepted 6 Nov 2011; published 7 Nov 2011

generating a binary mask and the center of mass of this mask corresponds to the center of the cell. As can be seen in the inset to Fig. 2a the red blood cell appears to be less circular than expected, this is due to the square aperture of the spatial light modulator (SLM) which is not large enough to allow all the high frequency components when a small numerical aperture objective is used. This problem can be overcome by adjusting the magnification of the SLIM system, using a higher NA objective or using a larger aperture SLM. For each cell a horizontal and vertical line profile are then measured through the center, for both the absorption and phase map (Fig. 2c). This approach assumes that the cells are radially symmetric, which is a reasonable approximation for red blood cells, although for future clinical work a pixel by pixel comparison will be ideal. From the phase profiles the peak values are chosen and from the intensity profile the minima are chosen. As can be seen in Fig. 2c, the phase and absorption profiles are in good agreement except for in the dimple region of the blood cell. For this reason, to demonstrate the feasibility of this technique just the peak values were chosen for the analysis presented here. Of course, for clinical translation, this mismatch must be understood and addressed. Figure 2d shows that the phase and absorption measurements are in fact linearly related and proves the feasibility of this approach.

The peak values from the horizontal and vertical profiles are averaged and plugged into Eq. (5) and Eq. (6) to calculate the un-calibrated concentration and thickness values. For this analysis it is assumed that the blood cells are oxygenated and we obtained the absorption spectrum for hemoglobin from Ref. [33]. The volume for each cell is calculated by multiplying the average thickness, calculated from the line profiles, by the projected area of the cell. For calibration, the measured mean cell volume (MCV) and mean cell hemoglobin concentration (MCHC) values are plotted against the values reported by the CBC and a best fit line is calculate to provide a calibration function. In principle this analysis could be completely automated as previously shown [10,21], but is not necessary for the proof of principle of this technology.

4. Results

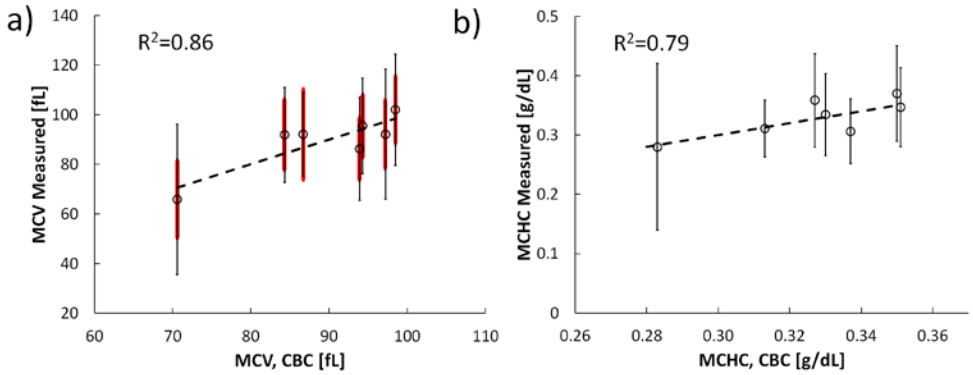

Fig. 3. Comparison of measured mean values with clinically reported values. (a) Mean Cell Volume, red error bars correspond to the SD reported by the Clinic and black error bars correspond to SD measured by the QPI and absorption measurements (b) Mean Cell Hemoglobin Concentration, error bars correspond to the measured SD, no SD information on the hemoglobin concentration is available from the Clinic. The dashed black lines have a slope of one.

For this study, samples from a total of 7 patients were measured and total of 651 cells were analyzed with an average of 93 cells per patient. The comparison between the calibrated mean values from our measurements and the CBC values is shown in Fig. 3. It can be seen that both the measured MCV and MCHC agree well, with R^2 values of 0.86 and 0.79, respectively. The discrepancies are likely due to two major reasons. First, the MCHC reported by the clinic is

#155401 - $15.00 USD Received 27 Sep 2011; revised 21 Oct 2011; accepted 6 Nov 2011; published 7 Nov 2011

calculated by lysing all the blood cells to make a solution of hemoglobin. An absorption measurement is then made on this solution to calculate the hemoglobin concentration.

Therefore, this measurement doesn't take into account any variability in hemoglobin concentration between cells. Secondly, the number of cells measured in this study is relatively low compared to the large numbers measured by the clinical impedance counters. Since the comparison between our measurements and the clinic relies on calibration, the agreement will likely increase with an increase in throughput.

For the volume measurement, Fig. 3a also shows the standard deviations measured by the clinic in red and those measured by our technique in black. The lack of perfect agreement in the distribution widths is most likely due to the higher sensitivity of our method and the difference in the sample sizes measured. Although the clinical counter we are comparing our measurement to, does provide a histogram of size distributions for each patient, it does not have the capability to do the same for hemoglobin concentration, Fig. 3b thus only shows the standard deviations in the hemoglobin concentration distributions measured by our technique. The fact that the clinical analyzer in a major community hospital does not have this capability illustrates the need for a simple approach to provide this measurement.

5. Discussion and conclusions

In this study we have shown both theoretically and experimentally that by combining quantitative phase measurements with bright field absorption measurements it is possible to calculate both cell morphology and hemoglobin concentration at a single cell level. The method was validated by comparing the values measured with those reported by a state of the art automated clinical blood analyzer. Although in this study a calibration was necessary, in the future a more detailed understanding of the formation of the bright field image may render this step unnecessary. In particular, the measured intensity includes contributions from scattered light and is not a pure absorption map as described by Beer's law. Furthermore Lambert-Beer's law must be rewritten for the case of convergent illumination as is provided by a typical microscope. The fact that the phase and absorption are linearly related, without taking these effects into account, indicates that the contribution from them is constant for red blood cells.

Although we used SLIM to measure phase, in principle this technology could be utilized in combination with any QPI method. However, SLIM is well suited for this method since it does not require any modifications to a commercial microscope and the filter wheel required for the absorption measurements may easily be integrated with the white light illumination. The fact that SLIM requires 4 intensity measurements is only a practical issue as the advent of fast spatial light modulators, cameras and scanning software means that the speed of the measurement may easily be increased. Furthermore, the high SNR provided by SLIM ensures that data analysis technology can easily be automated to increase throughput. Since SLIM can simply be added as a modality to an existing microscope, minimal re-training will be necessary to use the equipment especially given that the parameters provided by this analysis are already familiar to pathologists and technicians.

In conclusion, the technology presented here offers a powerful new blood screening tool that may aid pathologists in making differential diagnosis and risk stratification. This technology combined with the morphological analysis described previously [10,21] provides the ability to analyze red blood cells with unprecedented details and may enable new diagnostic capabilities when monitoring and treating red blood cell disorders. Furthermore, the ability to easily measure single cell hemoglobin concentrations may open new avenues for monitoring blood cell disorders and the effects of treatment.

Acknowledgments

This research was supported in part by the National Cancer Institute (R21 CA147967-01) and the National Science Foundation (grants CBET 08-46660 CAREER, CBET-1040462 MRI, CBET-0939511). For more information, visit http://light.ece.uiuc.edu/.

#155401 - $15.00 USD Received 27 Sep 2011; revised 21 Oct 2011; accepted 6 Nov 2011; published 7 Nov 2011